Characterisation of Quorum Sensing System and Its Role in Global Regulation in *Hafnia alvei*

Jia Yi Tan[1,2], Wah-Seng See-Too[1], Peter Convey[3], Kok-Gan Chan[1,2]*

Author affiliations:
[1] Division of Genetics and Molecular Biology, Institute of Biological Sciences, Faculty of Science, University of Malaya, Kuala Lumpur 50603, Malaysia;
[2] International Genome Centre, Jiangsu University, Zhenjiang 212013, PR China;
[3] British Antarctic Survey, NERC, High Cross, Madingley Road, Cambridge CB3 OET, UK

***Correspondence**: Kok-Gan Chan, kokgan@um.edu.my

Keywords: Genomic, Transcriptomic, RNA-seq, Quorum sensing, *Hafnia alvei*

Abstract: Quorum sensing (QS) is a regulatory process achieved *via* cell-to-cell communication that involves release and detection of autoinducers (AIs), and which occurs in a wide range of bacteria. To date, QS has been associated with events of pathogenesis, biofilm formation, and antibiotic resistance in clinical, industrial, and agricultural contexts. The main objective of this study was to characterise the role of *N*-Acyl homoserine lactone (AHL) type QS in *Hafnia alvei* FB1, a bacterial strain isolated from frozen vacuum-packed fish paste meatballs, via identification of QS core genes using a genomic approach, followed by comparative transcriptomic profiling between QS-deficient mutants and wild-type strains. *H. alvei* FB1 is known to produce two types of AHLs, namely, *N*-(3-oxohexanoyl) homoserine lactone (3OC6-HSL) and *N*-(3-oxooctanoyl) homoserine lactone (3OC8-HSL). The complete genome sequence of strain FB1 was obtained and a single gene for AHL synthase (*halI*) and its cognate receptor (*halR*) were identified. QS-deficient mutants of FB1 were constructed via the λ-Red recombineering method. Removal of the QS genes in strain FB1 affected mainly mechanisms in cell division and nutrient uptake, as well as resistance to a number of antibiotics, which are crucial for survival, adaptation and colonisation of both food and the host gut environment.

Impact statement: Members of the genus *Hafnia* are known as opportunistic pathogens in both nosocomial and community-acquired infections. However, the involvement and mechanism of pathogenesis of *Hafnia* in infectious diseases remains uncertain. We investigatd the role of the signalling molecule group, *N*-acyl homoserine lactones (AHLs), in a *Hafnia alvei* strain, since AHLs play important roles in pathogenicity, survival or adaptation in other pathogens. The comparative transcriptomic study revealed that AHLs are involved in mechanisms in cell division and nutrient uptake, as well as resistance to a number of antibiotics, which are crucial for survival, adaptation and colonisation of both food and the host gut environment. These findings provide insight into possible strategies to combat this opportunistic pathogen.

Data summary: Genome sequence is deposited in NCBI GenBank under accession number CP009706. The transcriptomic data have been deposited in the Gene Expression Omnibus (GEO) database (https://www.ncbi.nlm.nih.gov/gds) under accession number GSE93000.

Introduction

Quorum sensing (QS) is a form of cell-to-cell communication expressed by a wide range of bacterial species, achieved by the release and detection of signaling molecules called autoinducers (AIs) (1). *N*-acyl-homoserine lactone (AHL) is one such type of molecule, commonly produced by Proteobacteria. Individual cells monitor the changes in 'quorum' through detection of these small, often lipophilic, molecules in the environment and, in response, adjust the expression of a network of genes in a collective manner (2). AHL-based QS has been reported to be associated with various microbial activities of clinical, industrial, and agricultural importance, such as regulation of virulence expression (3-5), production of antibiotics (6, 7), biofilm formation (8-10), and food spoilage (11-13).

Hafnia, a bacterial genus characterised by rod-shaped, motile, flagellated and facultatively anaerobic cells, belongs to the family *Hafniaceae*. *Hafnia alvei* has been identified to be among the enteric bacteria commonly involved in food spoilage (11, 12, 14, 15), and also as an opportunistic pathogen (16). The ability of *H. alvei* to survive at low temperature (15) has made it an interesting subject of study in controlling bacterial contamination in the food industry. Despite the common association of *H. alvei* with human gut microbiota (17-19), its status as a gut pathogen is still uncertain. Therefore, it is also important to confirm whether this common microbial contaminant of food could also be a source of gut infection.

The focus of this study, *H. alvei* FB1 is an AHL-producing strain recovered from vacuum-packed refrigerated fish paste meatballs (commonly known as 'fish ball'). We have previously confirmed that the strain produces two oxo-AHLs with side chains of six or eight carbons in length (20).

In recent years, advancement in high-throughput sequencing and accessibility of powerful bioinformatics pipelines have enabled bacterial genomes and transcriptomes to be explored with increasing ease. Further, current DNA recombinant technology allows precise genome editing and provides a convenient tool in the study of QS regulons. This study investigated the genetic basis of AHL-based QS signalling in *H. alvei* FB1, as well as the regulatory role of QS in *H. alvei,* by studying the QS-deficient mutants in a comparative transcriptomics context.

Methods

Bacterial Strains, Plasmids and Culturing Conditions

All bacterial strains and plasmids used in this study are listed in Table 1 along with their relevant characteristics. All strains were cultured and maintained in Luria-Bertani (LB) medium. Unless stated otherwise, the growth temperatures for *Chromobacterium violaceum* CV026, *Escherichia coli* and *H. alvei* strains were 28°C, 37°C and 30°C, respectively.

91 **Whole Genome Sequencing**
92
93 The gDNA used in this study was extracted with the MasterPure™ DNA Purification Kit
94 (Epicentre, USA) following the manufacturer's protocol. The quality of gDNA extracted was
95 assessed according to "PACBIO® GUIDELINES FOR SUCCESSFUL SMRTbell™ LIBRARIES" prior
96 to library preparation for sequencing. Preparation of SMRTbell template libraries was carried
97 out with SMRTbell Template Prep Kit 1.0 (Pacific Biosciences, USA) following the
98 manufacturer's protocol for 20 kb template preparation. SMRT sequencing was performed
99 using a PacBio RSII Sequencer (Pacific Biosciences, USA) with 3 SMRT cells.
100
101 Quality filtering and *de novo* assembly of the output reads were performed using the
102 Hierarchical Genome Assembly Process (HGAP) pipeline version 3.0 on the Pacific Biosciences'
103 SMRT portal (21). Polished assemblies were generated from this module that incorporated
104 Celera Assembler, BLASR mapper, and Quiver consensus caller algorithms. The assembled
105 genome sequence was then annotated by SEED-based subsystem characterisation on the
106 RAST server (22, 23) and Prokaryotic Genome Automatic Annotation Pipeline (PGAAP) (24).
107
108 **Identification of QS genes from the annotated data**
109
110 Candidates of potential *luxI* and *luxR* homologues were identified from the annotated
111 genome with the 'BLAST search' function on RAST. A search on the Conserved Domain
112 Database (CDD) (25) was performed to identify the signature conserved domains on the
113 candidate sequences. The sequences were aligned with other known homologues obtained
114 from the GenBank database (https://www.ncbi.nlm.nih.gov/) and visualised using Jalview
115 version 2. Phylogenetic analysis was performed using SeaView version 4 (26).
116
117 **Cloning and Expression of the *luxI* homologue**
118
119 Identity and function of the *luxI* homologue were determined via cloning and expression
120 study using Gene Synthesis service (GenScript, USA). The target DNA sequence was first
121 synthesised in vector pUC57, and then sub-cloned into *E. coli* expression vector pGS21a by
122 the service provider. The expression vector carrying the target sequence was transferred into
123 expression host *E. coli* BL21 Star (DE3). The expression of the *luxI* homologue was examined
124 *via* a cross-streak assay on the transformed host with a CV026 biosensor. AHLs produced were
125 then identified on an LC-MS/MS platform as described previously (20).
126
127 **Construction of *halI* and *halR* replacement knockout mutants**
128
129 Replacement knockout of QS genes in *H. alvei* FB1 was carried out according to Court Lab's
130 protocol "Recombineering: Using Drug Cassettes to Knock out Genes *in vivo*", downloadable
131 from the official website (https://redrecombineering.ncifcrf.gov/). Linear DNA substrates for
132 recombineering were constructed through PCR amplification with 70-base hybrid primers
133 (Table 2) consisting of 50 bases of homologous sequence that flanked the sequence to be
134 replaced and 20 bases at the 3' end that primed the amplification of the kanamycin resistance
135 (KanR) cassette from the template strain (TKC) (27). The substrates were later introduced into
136 heat-induced *H. alvei* FB1 cells harbouring pSIM7 *via* electroporation, in which the
137 recombinases were actively expressed. The recovered cells were then plated on a kanamycin

138 plate (35 µg/mL) to select for mutants that carried the KanR cassette in the place of QS genes.
139 The results of recombineering were then confirmed by colony PCR using primers (*hslI*_u-F,
140 *hslI*_d-R, *halR*_u-F, and *halR*_d-R with Screen_KanR-F and Screen_KanR-R, as described in
141 Table 2) that amplified the junctions where recombination took place. Cross-streaking with
142 CV026 was also performed on the *H. alvei* FB1Δ*hslI*::KanR to confirm that the AHL synthase
143 function had been successfully removed.
144
145 **RNA-Seq**
146
147 *H. alvei* FB1 WT and mutant cells were grown in 200 mL LB broth at 30°C with shaking at 220
148 rpm. Readings of optical density (OD_{600}) were taken every hour. The total RNA was stabilised
149 immediately using Qiagen RNAprotect bacterial reagent (Qiagen, USA) when the cells were
150 harvested at the desired OD_{600} (0.5 and 1.5), following the manufacturer's protocol. Total
151 bacterial RNA was purified using the Qiagen RNeasy kit (Qiagen, USA) following the
152 manufacturer's protocol. Purified RNA samples were eluted in 100 µL sterile RNase-free
153 water. Total RNA from three biological replicates was obtained from independent cultures to
154 evaluate the reproducibility of RNA-Seq data. Purity of RNA samples was assessed using a
155 Nanodrop spectrophotometer (Thermo Scientific, USA), and RNA quantification was carried
156 out using the Qubit® RNA HS Assay Kit (Invitrogen, USA). The quality of the extracted RNA
157 samples was assessed with an Agilent RNA 6000 Nano Kit (Agilent Technologies, USA) using a
158 2100 Bioanalyzer.
159
160 RNA samples with RNA Integrity Number (RIN) >7.0 were chosen to proceed to rRNA
161 depletion using Ribo-Zero™ rRNA Removal Kits (Bacteria) (Epicentre, USA) prior to cDNA
162 synthesis. The quality of the rRNA-depleted RNA was assessed with an Agilent RNA 6000 Pico
163 Chip (Agilent Technologies, USA) using a 2100 Bioanalyzer. Library preparation was
164 performed following the manufacturer's protocol using the Illumina ScriptSeq™ v2 RNA-Seq
165 Library Preparation Kit (Epicentre, USA). Quality of the RNA-Seq transcriptome library was
166 examined using Agilent 2100 High Sensitivity DNA Kit. Quantification of the library was
167 assessed using the Qubit® dsDNA HS Assay Kit (Life Technologies, USA) and qPCR (KAPA
168 Biosystems) before being subjected to normalisation. The normalised samples (4 nM) were
169 denatured with 0.2 N NaOH and diluted 20 pM using pre-chilled Hybridisation Buffer (HT1)
170 (Illumina, USA). The 20 pM transcriptome libraries were further diluted to 10 pM with pre-
171 chilled HT1 buffer prior to whole transcriptome sequencing on a MiSeq platform.
172
173 RNA-seq read quality assessment was carried out using FastQC (version 0.11.2) (28).
174 Rockhopper (29, 30) was used to align the paired end reads against the *H. alvei* FB1 reference
175 genome (GenBank accession number CP009706). Differential expression analysis was then
176 performed with the DESeq2 package using the raw counts generated from Rockhopper as
177 inputs (p_{adjust} value/$q < 0.01$) (31). Gene Ontology (GO) and pathway enrichment analyses of
178 differentially expressed genes (DEGs) were performed using The Database for Annotation,
179 Visualization and Integrated Discovery (DAVID) v6.8 (32, 33)
180
181 **qPCR**
182
183 Prior to qPCR, total RNA was converted to cDNA using the QuantiTect® Reverse Transcription
184 Kit (Qiagen, Germany) following manufacturer's protocol. qPCR was performed with a CFX96

Touch™ Real-Time PCR Detection System (Bio-Rad, USA) using the primers listed in Table 2. Expression levels in ΔΔCq of each gene were determined from analyses using Bio-Rad CFX Manager version 3.1 (Bio-Rad, USA).

Results

Identification of QS genes of *H. alvei*

The genome sequence of *H. alvei* FB1 is deposited in GenBank under the accession number CP009706. A homology search using LuxI and LuxR amino acid sequences via the 'BLAST search' function on the RAST server revealed the presence of a pair of open reading frames (ORF) at position 2,668,370 – 2,669,738 in the genome that contained the signature conserved domains of LuxI and LuxR homologues. The pair consisted of a 648-bp *halI* (Locus tag AT03_RS12360) along with a 741-bp *halR* (AT03_RS12355). The pair was in convergent orientation, with a 20-bp overlap at the 3'-ends (Figure 1A).

Multiple sequence alignment (MSA) was performed between HalI amino acid sequence and other known homologues of LuxI (Figure 1B). Ten conserved key amino acid residues, namely R25, F29, W35, E44, D46, D49, R70, F84, E101 and R104 according to their positions in TraI as reported by Fuqua and Greenberg (34), were identified in the sequence of HalI. Likewise, MSA on HalR and other known homologues of LuxR revealed the presence of six conserved key residues (W57, Y61, D70, P71, W85 and G113 according to their positions in TraR) within the autoinducer binding domain and three (E178, L182, and G188) within the DNA binding domain (Figure 1C), as reported by Subramoni et al. (35).

Phylogenetic trees were built to illustrate the phylogenetic relationships between the HalI and HalR proteins and other LuxI and LuxR homologues of known functions (Figures 1, 2). Both trees shared roughly similar topologies, consisting of two major clusters. The top clusters consisted solely of members of γ-Proteobacteria, whereas the bottom ones contain those of α-, β- and γ-Proteobacteria. All sequences from *Hafnia* spp. formed a single clade in both trees, except for an orphan LuxI homologue (YspR) in *H. paralvei* bta3-1 that clustered with the more distantly related SmaR of *Serratia* sp. ATCC 39006. Both HalI and HalR were more closely related to YspI-YspR in *Yersinia pestis* and YtbI-YtbR in *Y. pseudotuberculosis*, compared with *Edwardsiella tarda* ATCC 15947^{T} that also belongs to the *Hafniaceae*. The LuxR tree clearly shows that all the HalR sequences formed a monophyletic clade with the sequences of LuxR homologues that are known to establish quorum-hindered activities.

Expression of *halI* in a Foreign Host

To prove the functionality of the identified AHL synthase, the *halI* sequence was cloned into a pGS-21a vector and expressed in host *E. coli* BL21 Star (DE3). Cross-streaking of the transformed BL21 Star (DE3) induced purple pigmentation of the CV026 biosensor (Figure S1). The same AHL profile produced by *H. alvei* FB1 (3OC$_6$-HSL and 3OC$_8$-HSL) was detected using LC-MS/MS (Figure S2).

Mutant Construction *via* λ-Red Recombineering

232 Two mutants, namely, Δ*halI*::kanR and Δ*halR*::kanR were constructed using the λ Red
233 recombineering technique. In each mutant, either *halI* or *halR* was replaced with a kanamycin
234 resistance cassette. Verification of the mutants was performed via PCR on colonies picked
235 from LBA plates containing 35 mg/mL kanamycin. The presence of amplification products
236 encompassing the junctions between the flanking regions and a stretch of the intragenic
237 region of KanR cassette indicated the success of the replacement knockout. The PCR products
238 were sent for Sanger sequencing to confirm the sequences (Figure S3). The Δ*halI*::kanR
239 mutants, when tested by cross-streaking with biosensor CV026, were unable to induce purple
240 pigment production (Figure S4).
241
242 **RNA-Seq**
243
244 To examine the pattern of global gene expression affected by HalR regulon, RNA-Seq was
245 performed for the two mutants using strain FB1 WT as a control. Transcriptomes of each
246 strain were acquired at early- and mid-exponential phase (OD_{600} = 0.5 and 1.5, respectively).
247 Three libraries of FB1 WT, Δ*halI*::KanR, and Δ*halR*::KanR were generated for each growth
248 phase, which yielded total reads ranging from 2,124,060 to 4,957,038. The Rockhopper
249 software was able to map between 504,685 and 3,344,049 reads to the reference genome.
250 The sequencing output, along with the raw counts, have been deposited in the Gene
251 Expression Omnibus (GEO) database (https://www.ncbi.nlm.nih.gov/gds) under accession
252 number GSE93000.
253
254 **Quality Assessment of the Replicates**
255
256 The principal component analysis (PCA) plot based on the raw counts showed that, for the
257 samples harvested at OD_{600} 0.5, the three replicates of Δ*halR*::KanR samples were clearly
258 separated from the WT and Δ*halI*::KanR samples along the PC1 axis, which contributed
259 94.662% of the variation, while the latter two clustered close to each other on this axis (Figure
260 3A). For the samples harvested at OD_{600} 1.5, the replicates formed distinct clusters in different
261 quadrants of the plot, with the Δ*halI*::KanR mutant forming a cluster more distinct from the
262 WT samples along the PC1 axis (which explained 79.838% of variation) than the Δ*halR*::KanR
263 samples (Figure 3B).
264
265 **Transcriptomic Analysis of QS Mutants**
266
267 No significant differential expression ($\log_2$ fold change [FC] > 1 or < -1) was observed in the
268 Δ*halI*::KanR mutant at a *q*-value of 0.01, aside from *halI*. A total of 687 genes were found to
269 be differentially expressed in the Δ*halR*::KanR mutant, of which 511 were up-regulated
270 while 176 were down-regulated. The distribution of DEGs is illustrated as MA plots in Figure
271 4A, B.
272
273 A total of 825 and 740 genes were differentially expressed in the Δ*halI*::KanR and Δ*halR*::KanR
274 mutants, respectively. In the former, 392 were up-regulated while 433 were down-regulated,
275 while in the latter, 371 showed positive fold-changes against the WT strain while 369 showed
276 negative. The distribution of DEGs is illustrated as MA plots in Figure 4C, D, and the
277 overlapping genes between both mutants are shown in Venn diagrams (Figure 5)
278 FC of genes in each experimental condition are listed in Table S1.

279 For the Δ*halR*::Kan mutant in exponential phase, both up- and down-regulated gene lists were
280 topped by genes involved in carbohydrate transport and metabolism. Up-regulated genes
281 were mainly involved with ribose metabolism, whereas down-regulated genes involved in
282 mannitol, maltose and galactose uptake were among those with the highest FCs. In mid-
283 exponential phase, genes involved in amino acid transport and metabolism were most
284 abundant in the lists of both mutants. Genes involved with maltose transport, for instance
285 maltoporin, which were down-regulated in the early exponential phase, were up-regulated in
286 the mid-exponential phase.
287
288 **GO and Pathway Enrichment Analysis of QS-dependent Genes**
289
290 GO enrichment analysis was performed on the DEGs to gain an insight into the QS-regulated
291 genes. At the early exponential phase, out of the 511 up-regulated genes in the Δ*halR*::KanR
292 mutant, 438 were assigned to 197 GO terms, of which five terms were enriched (*q*-value <
293 0.01). Of the 176 down-regulated genes, 114 were assigned to 58 terms, of which only two
294 were enriched (Figure 6). The GO terms enriched in the up-regulated DEGs included fatty acid
295 biosynthetic processes, cytoplasm, ATP binding, RNA binding, and tRNA binding, whereas the
296 down-regulated genes included those involved in the phosphoenolpyruvate-dependent sugar
297 phosphotransferase system and in response to stress.
298
299 In the mid-exponential phase, 304 out of 371 up-regulated genes in the Δ*halR*::KanR mutant
300 were assigned to 180 GO terms, and two (phosphoenolpyruvate-dependent sugar
301 phosphotransferase system and cobalamin biosynthesis process) were significantly enriched.
302 Of the 263 GO terms accounting for 317 of the 369 down-regulated genes, only one (TCA
303 cycle) was significantly enriched. In the *halI* mutant, genes with positive and negative FCs
304 were assigned to 132 and 138 GO terms, respectively. None of these terms were enriched at
305 *q*-value = 0.01.
306
307 DEGs were also mapped into the KEGG pathway database to identify pathways that were
308 significantly enriched in each experimental condition (Figure 10). In early exponential phase,
309 the up-regulated genes in the Δ*halR*::KanR mutant were assigned to a total of 80 pathways,
310 of which 12 were significantly enriched at the cut-off of *q*-value = 0.01. These pathways
311 included primarily those involved in biosynthesis of molecules and functions that involved
312 nucleotides. Six of the 59 pathways to which the down-regulated genes in the Δ*halR*::KanR
313 mutant were assigned were significantly enriched. As in the GO ontology, the
314 phosphotransferase system (PTS) was involved, along with several other pathways involved
315 in carbohydrate metabolism.
316
317 In mid-exponential phase, the number of down-regulated pathways in the Δ*halR*::KanR
318 mutant far exceeded those that were up-regulated. A total of 30 out of 80 pathways were
319 significantly enriched. These pathways were mostly involved in amino acid metabolism. The
320 Δ*halI*::KanR mutant in the same growth phase showed a much smaller number of enriched
321 pathways than did the Δ*halR*::KanR, but they were still dominated by down-regulated genes.
322 Most of these pathways overlapped those affected in the *halR* counterpart, except for beta-
323 lactam resistance.
324
325 **Validation of RNA-Seq Data by qPCR**

To validate the RNA-Seq results, six genes were randomly chosen for qPCR. The $\log_2$ FCs of qPCR were calculated and plotted against that of RNA-Seq (Figure 8). The correlation coefficients were all above 0.99, indicating that the results obtained were reliable

Discussion

Having examined *in silico* the characteristics of the candidates of QS genes in *H. alvei* FB1, the strain, unlike some other members of Proteobacteria, possessed only a single pair of *luxI-luxR* homologues. The presence of conserved domains and amino acid sites that are signature to the group of proteins, along with the orientation of the genes, provide strong evidence supporting the identity of the QS gene candidates. Phylogenetic trees constructed using choices of sequences included in the analyses adapted from a review by Tsai and Winans (36) revealed that the amino acid sequences of HalR proteins obtained from members of the genus *Hafnia* fell into a monophyletic clade with other EsaR-like proteins. This, along with other traits, such as a convergent orientation with overlapping 3'-ends and responding to $3OC_6$-HSL, suggested the possibility that HalR might establish similar quorum-hindered behaviour. An intermingling pattern between sequences originating from genomes that belonged to different classes of Proteobacteria was observed in one of the major clusters in both phylogenetic trees. This observation, along with the distant phylogenetic relationship between the orphan LuxR homologue with HalR, is likely to reflect the occurrence of HGT in the past, as has been reported in previous studies (37, 38).

According to the results of the transcriptomic study, Δ*halI*::KanR and Δ*halR*::KanR mutants showed difference in the functional distribution patterns of DEGs, which supports the proposition that HalR proteins belong to the quorum-hindered group. At early exponential phase, no significant DEG was observed in Δ*halI*::KanR, whereas a large number of DEGs were found in Δ*halR*::KanR. We suggest that, at OD_{600} of 0.5, the concentration of AHLs within the culture environment was still too low to affect the expression of any genes. Therefore, the mutant lacking AHL-synthase established a gene expression profile similar to the WT strain. The observation that removal of the *halR* gene resulted in a very different expression profile pointed to the possibility that there were HalR proteins already binding at the promoter regions of certain genes at this early stage, playing a regulatory role in the absence of sufficient QS signals. A much larger number of up-regulated genes was observed in the Δ*halR*::KanR mutant compared with those that were down-regulated, indicating that the major role of the HalR protein at this stage could be repression of certain functions in an early growth phase.

Later, in the mid-exponential phase, the gene expression profiles in the two mutants changed. As illustrated by PCA, the Δ*halR*::KanR mutant now clustered closer to the WT strain, implying that, with the increasing concentration of AHL molecules over time, the HalR proteins in FB1 WT were then released from their binding sites and the expression levels of the previously repressed genes became similar to the unrepressed ones in Δ*halR*::KanR. At this stage, DEGs could also be observed in the Δ*halI*::KanR mutant. More than half of these genes showed changes in the same directions in both mutants, which reflected a scenario more complex than classical examples of 'quorum-hindered apo-proteins', in which the changes in both

372 mutants were expected to be in opposite directions. This observation suggests that a more
373 complicated regulatory mechanism could be involved in the QS system in *H. alvei*.
374
375 **Functional Distribution of QS-regulated Genes**
376
377 The enrichment analyses revealed that, in the early exponential phase, a number of traits
378 related to dormancy and survival under stressful conditions were affected by the removal of
379 the *halR* gene. The four GO terms most significantly enriched for up-regulated genes in the
380 exponential phase (cytoplasm, RNA binding, ATP binding, and tRNA binding) contained DEGs
381 that could be generalised into three categories: DNA replication (helicases, gyrase, and
382 topoisomerase), mismatch repair (*mutS*), and protein biosynthesis (rRNA and tRNA
383 methyltransferases, aminoacyl-tRNA synthetases), corresponding to the enriched KEGG
384 pathways (Aminoacyl-tRNA biosynthesis, DNA replication, Mismatch repair, and Protein
385 export)(Figure 7). Genes involved in metabolism of ribose, an important building block of DNA
386 and RNA backbones, were amongst the genes with the highest FCs. This up-regulation
387 occurring in the absence of HalR indicated that metabolism of nucleic acids was highly
388 repressed in WT cells. Fatty acid biosynthesis was also amongst the up-regulated functions in
389 both analyses, suggesting that the cell membrane biosynthesis was also repressed. Regulation
390 of chromosomal replication and cell division by QS has been reported in *E. coli* (39, 40) and *P.*
391 *aeruginosa* (41).
392
393 Genes involved in stress response and sugar uptake were negatively affected in the
394 Δ*halR*::KanR mutant, which could be reflected in the down-regulation of two biological
395 process terms (stress response and phosphoenolpyruvate-dependent sugar
396 phosphotransferase system) and five pathways (phosphotransferase systems, carbon
397 metabolism, microbial metabolism in diverse environments, fructose and mannose
398 metabolism, and citrate cycle). Several genes involved in PTS with specificity towards
399 mannitol and ascorbate, along with a number of other sugar permeases and transporters,
400 such as maltose, fructose, and galactose, were amongst the genes with significant FC.
401
402 In the mid-exponential phase, the expression profile in the Δ*halR*::KanR mutant changed
403 drastically. At this stage, many pathways involved in amino acid and fatty acid metabolism
404 were down-regulated. In other words, these pathways were expressed at a higher level in the
405 WT strain compared with the mutants, indicating that quorum sensing played a significant
406 role in promoting metabolic activities in *H. alvei* FB1. The results of the GO enrichment
407 analysis implied that phosphotransferase systems that were activated in WT earlier were now
408 repressed, suggesting that these functions were more important in the early than in the mid-
409 exponential phase. PTS are known to work not only as carbohydrate transport and
410 modification systems in all phyla of bacteria, but also have regulatory roles in numerous
411 cellular functions (42). In *E. coli*, glucose-specific PTS was found to inhibit other non-PTS sugar
412 permeases influencing the availability of glucose *via* dephosphorylation of the EIIA subunit
413 (43). This phenomenon, termed "catabolite repression", contributes to the establishment of
414 a hierarchy of sugar utilisation, which allows bacteria to utilise energy sources in an
415 economical manner, as well as a regulatory circuit that acts according to nutrient availability
416 (44).
417

418 The overall picture gained from these observations is that QS appears to be involved in
419 repressing the functions involved in cell growth in an early growth phase, where the cells are
420 still in the process of recovery from stationary phase stress, in a typical 'quorum-hindered
421 apo-protein' manner. The repressed genes may then be re-activated at a later stage when the
422 DNA-bound apo-proteins are 'hindered' by the presence of AHL molecules at high cell density.
423 Apo-HalR, on the other hand, could positively regulate the stress response and sugar uptake
424 functions in the early exponential phase. PTS and various sugar transport systems that are
425 active at low cell density could provide a mechanism for detection of nutrient availability and
426 management of energy consumption. Whether these events of repression and activation are
427 interdependent or under separate regulatory control will require further studies to resolve.
428
429 The observation that both mutants shared more than half of their enriched pathways in mid-
430 exponential phase strongly suggests that QS regulation operated in a manner different to the early
431 exponential phase. In contrast with the expectation in a 'quorum-hindered apo-protein' model, very
432 few DEGs showed contradicting expression levels between the two mutants at this stage. Further
433 study is required to provide a strong basis for the understanding of the regulatory mechanism of the
434 HalR protein.
435
436 **Author statements**
437
438 **Authors and contributors**
439 JYT conceived and designed the experiments, performed the experiments, analysed the
440 data, wrote the paper, and prepared figures and/ or tables. WSST conceived and designed
441 the experiments, performed the experiments, and analysed the data. PC reviewed the
442 manuscript. K-GC supervised the project, contributed reagents/ materials/analysis tools. All
443 authors approved the manuscript.
444
445 **Conflicts of interest**
446 The authors declare that there are no conflicts of interest.
447
448 **Acknowledgements**
449 K-GC thanks the research grants from the University of Malaya (FRGS grant FP022-2018A,
450 PPP grant PG136-2016A, and HIR grant H-50001-A000027). PC is supported by NERC core
451 funding to the British Antarctic Survey's 'Biodiversity, Evolution and Adaptation' Team.
452
453 **References**
454 **Miller MB, Bassler BL**. Quorum sensing in bacteria. *Annu Rev Microbiol* 2001; 55:165-199.
455 2. **Parsek MR, Greenberg EP.** Acyl-homoserine lactone quorum sensing in Gram-
456 negative bacteria: a signaling mechanism involved in associations with higher
457 organisms. *Proc Natl Acad Sci U S A* 2000; 97:8789-8793.
458 3. **Duerkop BA, Ulrich RL, Greenberg EP.** Octanoyl-homoserine lactone is the cognate
459 signal for *Burkholderia mallei* BmaR1-BmaI1 quorum sensing. *J Bacteriol* 2007;
460 189:5034-5040.
461 4. **Hao G, Burr TJ.** Regulation of long-chain N-acyl-homoserine lactones in
462 *Agrobacterium vitis*. *J Bacteriol* 2006; 188:2173-2183.
463 5. **Pearson JP, Feldman M, Iglewski BH, Prince A**. *Pseudomonas aeruginosa* cell-to-cell
464 signaling is required for virulence in a model of acute pulmonary infection. I*nfect*
465 *Immun* 2000; 68:4331-4334.

466 6. **Barnard AM, Bowden SD, Burr T, Coulthurst SJ, Monson RE, Salmond GP**. Quorum
467 sensing, virulence and secondary metabolite production in plant soft-rotting
468 bacteria. *Philos Trans R Soc Lond B Biol Sci* 2007; 362:1165-1183.
469 7. **Pierson LS, Gaffney T, Lam S, Gong F**. Molecular analysis of genes encoding
470 phenazine biosynthesis in the biological control bacterium, *Pseudomonas*
471 *aureofaciens* 30-84. *FEMS Microbiol Lett* 1995; 134:299-307.
472 8. **Rivas M, Seeger M, Jedlicki E, Holmes DS**. Second acyl homoserine lactone
473 production system in the extreme acidophile *Acidithiobacillus ferrooxidans*. *Appl*
474 *Environ Microbiol* 2007; 73:3225-3231.
475 9. **Tomlin KL, Malott RJ, Ramage G, Storey DG, Sokol PA, Ceri H**. Quorum-sensing
476 mutations affect attachment and stability of *Burkholderia cenocepacia* biofilms. *Appl*
477 *Environ Microbiol* 2005; 71:5208-5218.
478 10. **Labbate M, Queck SY, Koh KS, Rice SA, Givskov M, Kjelleberg S**. Quorum sensing-
479 controlled biofilm development in *Serratia liquefaciens* MG1. *J Bacteriol* 2004;
480 186:692-698.
481 11. **Blana VA, Nychas GJ.** Presence of quorum sensing signal molecules in minced beef
482 stored under various temperature and packaging conditions. *Int J Food Microbiol*
483 2014; 173:1-8.
484 12. **Bruhn JB, Christensen AB, Flodgaard LR, Nielsen KF, Larsen TO, *et al.*** Presence of
485 acylated homoserine lactones (AHLs) and AHL-producing bacteria in meat and
486 potential role of AHL in spoilage of meat. *Appl Environ Microbiol* 2004; 70:4293-
487 4302.
488 13. **Christensen AB, Riedel K, Eberl L, Flodgaard LR, Molin S, *et al*.** Quorum-sensing-
489 directed protein expression in *Serratia proteamaculans* B5a. *Microbiology* 2003;
490 149:471-483.
491 14. G**ram L, Christensen AB, Ravn L, Molin S, Givskov M.** Production of acylated
492 homoserine lactones by psychrotrophic members of the Enterobacteriaceae isolated
493 from foods. *Appl Environ Microbiol* 1999; 65:3458-3463.
494 15. **Ridell J, Korkeala H.** Minimum growth temperatures of *Hafnia alvei* and other
495 Enterobacteriaceae isolated from refrigerated meat determined with a temperature
496 gradient incubator. *Int J Food Microbiol* 1997; 35:287-292.
497 16. **Janda JM, Abbott SL.** The genus *Hafnia*: from soup to nuts. *Clin Microbiol Rev* 2006;
498 19:12-18.
499 17. **Milani C, Ticinesi A, Gerritsen J, Nouvenne A, Lugli GA, *et al.*** Gut microbiota
500 composition and *Clostridium difficile* infection in hospitalized elderly individuals: a
501 metagenomic study. *Sci Rep* 2016; 6:25945.
502 18. **Carding S, Verbeke K, Vipond DT, Corfe BM, Owen LJ.** Dysbiosis of the gut
503 microbiota in disease. *Microb Ecol Health Dis* 2015; 26:26191.
504 19. **Jiang H, Ling Z, Zhang Y, Mao H, Ma Z, *et al*.** Altered fecal microbiota composition in
505 patients with major depressive disorder. *Brain Behav Immun* 2015; 48:186-194.
506 20. **Tan JY, Yin WF, Chan KG**. Quorum sensing activity of *Hafnia alvei* isolated from
507 packed food. *Sensors (Basel)* 2014; 14:6788-6796.
508 21. **Chin CS, Alexander DH, Marks P, Klammer AA, Drake J, *et al*.** Nonhybrid, finished
509 microbial genome assemblies from long-read SMRT sequencing data. *Nat Methods*
510 2013; 10:563-569.
511 22. **Aziz RK, Bartels D, Best AA, DeJongh M, Disz T, *et al.*** The RAST Server: rapid
512 annotations using subsystems technology. *BMC Genomics* 2008; 9:75.

513 23. **Aziz RK, Devoid S, Disz T, Edwards RA, Henry CS, *et al*.** SEED servers: high-
514 performance access to the SEED genomes, annotations, and metabolic models. *PLoS*
515 *One* 2012; 7:e48053.
516 24. **Angiuoli SV, Gussman A, Klimke W, Cochrane G, Field D, *et al*.** Toward an online
517 repository of Standard Operating Procedures (SOPs) for (meta)genomic annotation.
518 *OMICS* 2008; 12:137-141.
519 25. **Marchler-Bauer A, Bo Y, Han L, He J, Lanczycki CJ, *et al*.** CDD/SPARCLE: functional
520 classification of proteins via subfamily domain architectures. *Nucleic Acids Res* 2017;
521 45:D200-D203.
522 26. **Galtier N, Gouy M, Gautier C.** SEAVIEW and PHYLO_WIN: two graphic tools for
523 sequence alignment and molecular phylogeny. *Comput Appl Biosci* 1996; 12:543-548.
524 27. **Sharan SK, Thomason LC, Kuznetsov SG, Court DL**. Recombineering: a homologous
525 recombination-based method of genetic engineering. *Nat Protoc* 2009; 4:206-223.
526 28. **Andrews S.** FastQC: a quality control tool for high throughput sequence data. 2010.
527 Available online at: http://www.bioinformatics.babraham.ac.uk/projects/fastqc
528 29. **McClure R, Tjaden B, Genco C**. dentification of sRNAs expressed by the human
529 pathogen *Neisseria gonorrhoeae* under disparate growth conditions. *Front Microbiol*
530 2014; 5:456.
531 30. **Tjaden B**. De novo assembly of bacterial transcriptomes from RNA-seq data. *Genome*
532 *Biol* 2015; 16:1.
533 31. **Love MI, Huber W, Anders S.** Moderated estimation of fold change and dispersion
534 for RNA-seq data with DESeq2. *Genome Biol* 2014; 15:550.
535 32. **Huang dW, Sherman BT, Lempicki RA.** Bioinformatics enrichment tools: paths
536 toward the comprehensive functional analysis of large gene lists. *Nucleic Acids Res*
537 2009; 37:1-13.
538 33. **Huang dW, Sherman BT, Lempicki RA**. Systematic and integrative analysis of large
539 gene lists using DAVID bioinformatics resources. *Nat Protoc* 2009; 4:44-57.
540 34. **Fuqua C, Greenberg EP.** Listening in on bacteria: acyl-homoserine lactone signalling.
541 *Nat Rev Mol Cell Biol* 2002; 3:685-695.
542 35. **Subramoni S, Florez Salcedo DV, Suarez-Moreno ZR.** A bioinformatic survey of
543 distribution, conservation, and probable functions of LuxR solo regulators in
544 bacteria. *Front Cell Infect Microbiol* 2015; 5:16.
545 36. **Tsai CS, Winans SC.** LuxR-type quorum-sensing regulators that are detached from
546 common scents. *Mol Microbiol* 2010; 77:1072-1082.
547 37. **Hao Y, Winans SC, Glick BR, Charles TC.** Identification and characterization of new
548 LuxR/LuxI-type quorum sensing systems from metagenomic libraries. *Environ*
549 *Microbiol* 2010; 12:105-117.
550 38. **Gray KM, Garey JR**. The evolution of bacterial LuxI and LuxR quorum sensing
551 regulators. *Microbiology* 2001; 147:2379-2387.
552 39. **DeLisa MP, Wu CF, Wang L, Valdes JJ, Bentley WE.** DNA microarray-based
553 identification of genes controlled by autoinducer 2-stimulated quorum sensing in
554 *Escherichia coli. J Bacteriol* 2001; 183:5239-5247.
555 40. **Withers HL, Nordström K.** Quorum-sensing acts at initiation of chromosomal
556 replication in *Escherichia coli*. *Proc Natl Acad Sci U S A* 1998; 95:15694-15699.
557 41. **Wagner VE, Bushnell D, Passador L, Brooks AI, Iglewski BH.** Microarray analysis of
558 *Pseudomonas aeruginosa* quorum-sensing regulons: effects of growth phase and
559 environment. *J Bacteriol* 2003; 185:2080-2095.

42. **Galinier A, Deutscher J.** Sophisticated regulation of transcriptional factors by the bacterial phosphoenolpyruvate: sugar phosphotransferase system. *J Mol Biol* 2017; 429:773-789.
43. **Kotrba P, Inui M, Yukawa H.** Bacterial phosphotransferase system (PTS) in carbohydrate uptake and control of carbon metabolism. *J Biosci Bioeng* 2001; 92:502-517.
44. **Brückner R, Titgemeyer F.** Carbon catabolite repression in bacteria: choice of the carbon source and autoregulatory limitation of sugar utilization. *FEMS Microbiol Lett* 2002; 209:141-148.

599 **Table 1: Bacterial strains and plasmids used in this study**

Strains or plasmids	Description	Genotype	Source/Reference
Chromobacterium violaceum CV026	Biosensor that produce purple coloured pigment (violacein) in the presence of short chain AHLs	*cviI*::mini-Tn*5*	(McClean et al., 1997)
E. coli DH5α	Laboratory strain engineered to maximise transformation efficiency; host to pSIM7	F^- Φ80*lac*ZΔM15 Δ(*lac*ZYA-*arg*F) U169 *rec*A1 *end*A1 *hsd*R17 (rK^-, mK^+) *pho*A *sup*E44 λ– *thi*-1 *gyr*A96 *rel*A1	Invitrogen, USA
E. coli TKC	Laboratory strain engineered to carry multiple drug cassette that served as templates for recombineering substrates.	*tetA, cat, kan*	Court Lab (court@ncifcrf.gov)
Hafnia alvei FB1	Isolate from fish ball	WT	This study
Hafnia alvei FB1-Δ*halI*::*kan*	Mutant with AHL synthase gene replaced by a kanamycin resistance cassette	Δ*halI*::*kan*	This study
Hafnia alvei FB1-Δ*halR*::*kan*	Mutant with AHL receptor gene replaced by a kanamycin resistance cassette	Δ*halR*::*kan*	This study
pSIM7	pBBR1 expressing the λ-Red 'recombinase' genes	Gam, Exo, and Bet; Chloramphenicol resistance	Court Lab (court@ncifcrf.gov)

600

601

602

603 **Table 2:** Oligonucleotides used in PCR amplification for mutant construction.

Primers	**Sequence (5' – 3')**	**Annealing temperature (°C)**	**Length (-mer)**	**Reference**
halI-KanR-F	ATA GCA GGA CGC GAA AAA CAC CAG CCA TAG ATA ATA TGG ATA GTA ACT AAA ATG TAA TCA AGG TGA TGG ATA TGG ACA GCA AGC GAA CCG	72	90	This study
halI-KanR-R	AGT AAG CAA CGC CCG ACA AGC AAT AAG GTT GGG CGT TGA ACT TGA TCT TAT TAC ACC AAT GCA GGC GTA ATC AGA AGA ACT CGT CAA GAA G		91	This study
halR-KanR-F	GTA CTT TGC GCC CTG TAC TTA AGT GCA TGT TGT CAC TCA GAC ATG GGA AAT TGA ACG TCT AGG AGC CCA ATA TGG ACA GCA AGC GAA CCG	72	90	This study
halR-KanR-R	AGT CGG TGG TAT TCA GTC CCA GAT GGT TAA TTG GCC AAT GTC GAT AGC CGT TAC GCC TGC ATT GGT GTA ATC AGA AGA ACT CGT CAA GAA G		91	This study
*halI*_u-F	CCA GCC ATA GAT AAT ATG GA	50 (with Screen_KanR-R)	20	This study
*halI*_d-R	AGT AAG CAA CGC CCG ACA AG	50 (with Screen_KanR-F)	20	This study
*halR*_u-F	AAG TGC ATG TTG TCA CTC AG	50 (with Screen_KanR-R)	20	This study
*halR*_d-R	AGT CGG TGG TAT TCA GTC CC	50 (with Screen_KanR-F)	20	This study
Screen_KanR-F	CAC TGA GTT TCA CGA GGA CT		20	This study
Screen_KanR-R	TGA ACG CAC CGT TAA ATT CC		20	This study

604

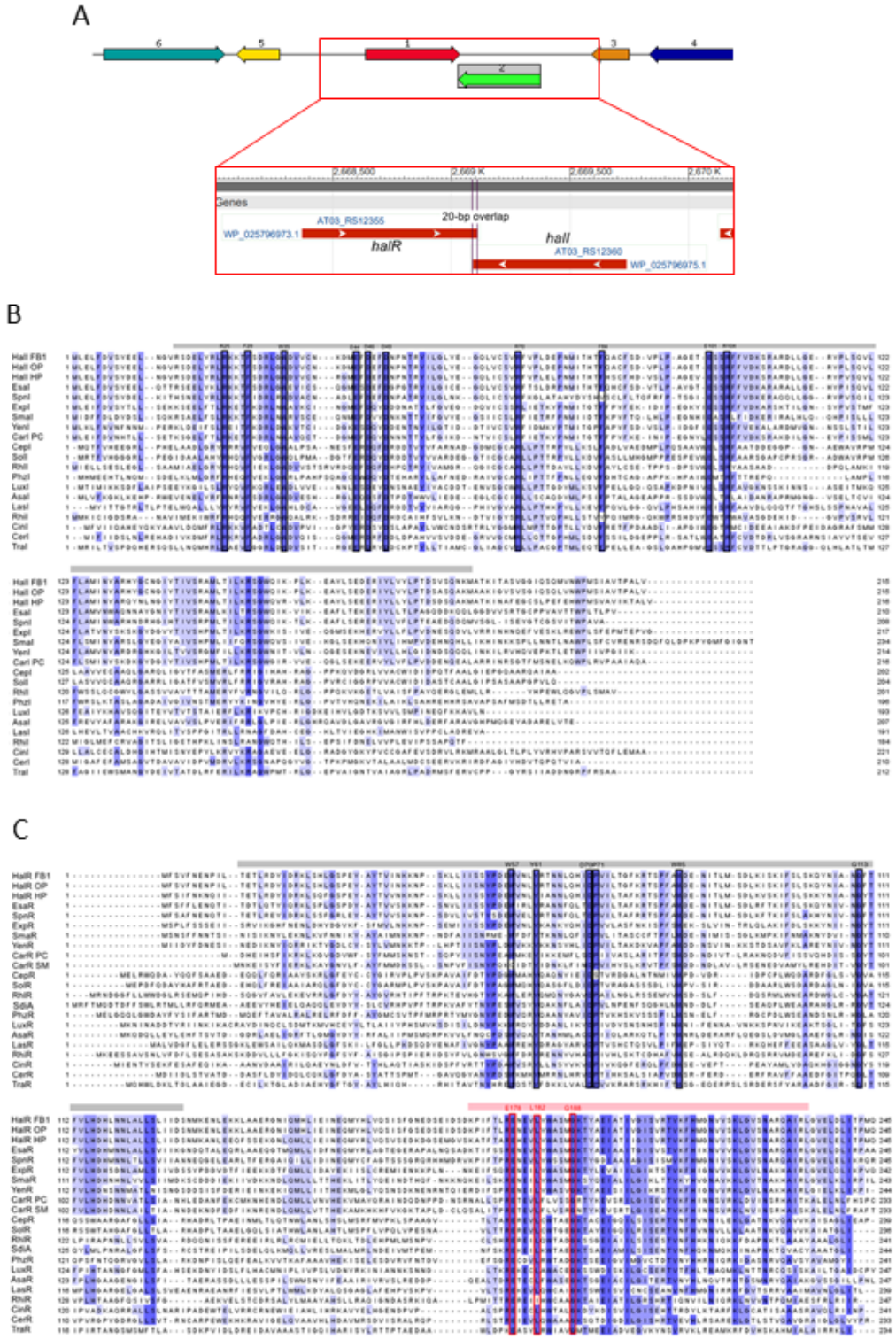

Figure 1: Physical map and sequence analyses of HalI and HalR in *H. alvei* FB1. (A) The arrows indicate the coding regions of *halI* and *halR*, along with the orientation and the flanking genes. 1. *halR*; 2. *halI*; 3. Hypothetical protein; 4. Probable secreted protein; 5. Permease of the drug/metabolite transporter (DMT) superfamily; 6. *umuC*. (B) MSA of amino acid sequences of HalI and other known LuxI homologues. Ten key conserved residues according to their positions in TraI are highlighted. OP: *O. proteus*; HP: *H. paralvei*; PC: *P. carotovorum*. (C) MSA of amino acid sequences of HalR and other known LuxR homologues. Nine key conserved residues within DNA binding domain according to their positions in TraR are highlighted. OP: *O. proteus*; HP: *H. paralvei*; PC: *P. carotovorum*.

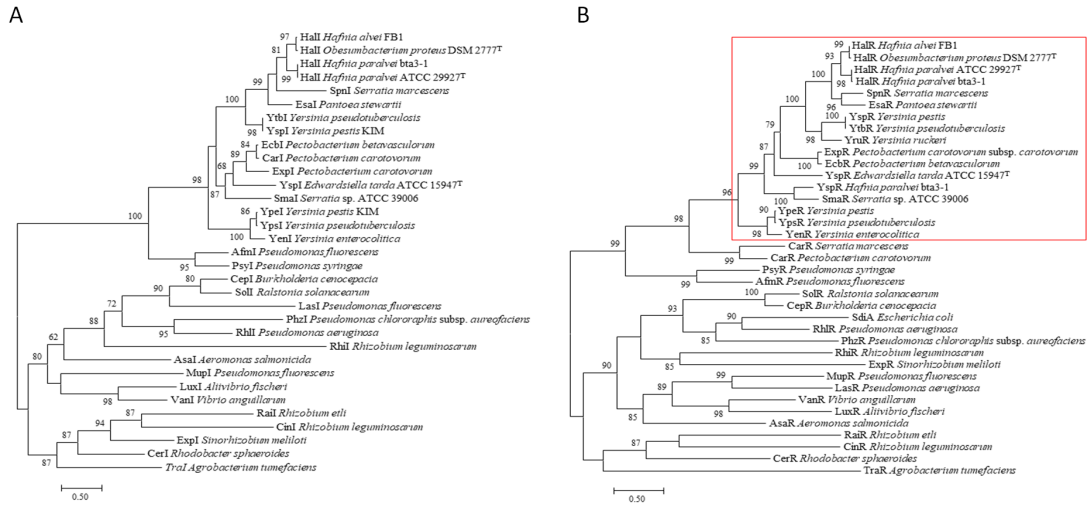

Figure 2: (A) Phylogenetic tree showing the evolutionary distance of HalI of *H. alvei* FB1 and other LuxI homologues inferred using the Maximum Likelihood (PhyML) method based on the LG matrix-based model. The tree with the highest log likelihood (-11301.6) is shown. The aLRT branch support values are shown next to the branches. The tree is drawn to scale, with branch lengths measured in 0.5 substitutions per site (bar). (B) Phylogenetic tree showing the evolutionary distance of HalR of *H. alvei* FB1 and other LuxR homologues inferred using the Maximum Likelihood (PhyML) method based on the LG matrix-based model. The tree with the highest log likelihood (-14799.2) is shown. The aLRT branch support values are shown next to the branches. The tree is drawn to scale, with branch lengths measured in 0.5 substitutions per site (bar). The monophyletic clade that contained HalR and other LuxR homologues known to establish quorum-hindered properties is highlighted in the red box.

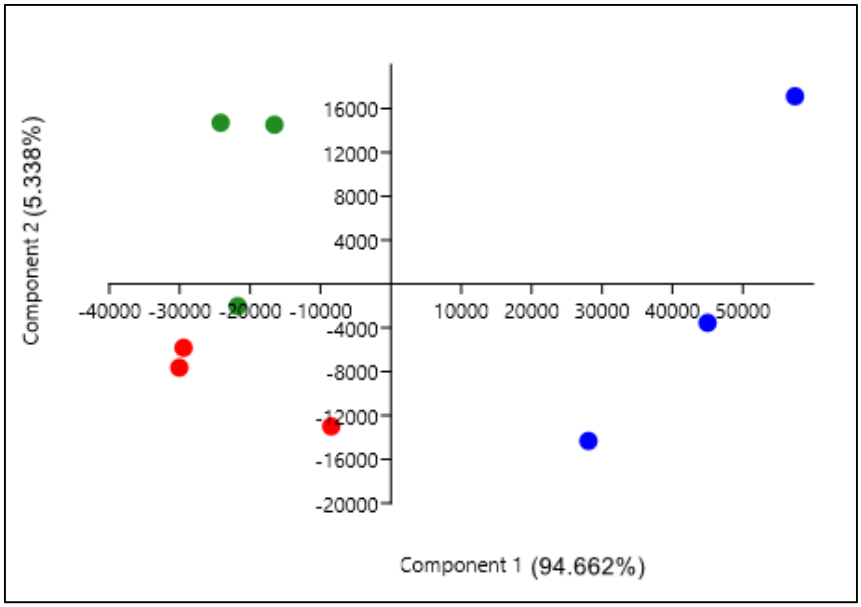

(A)

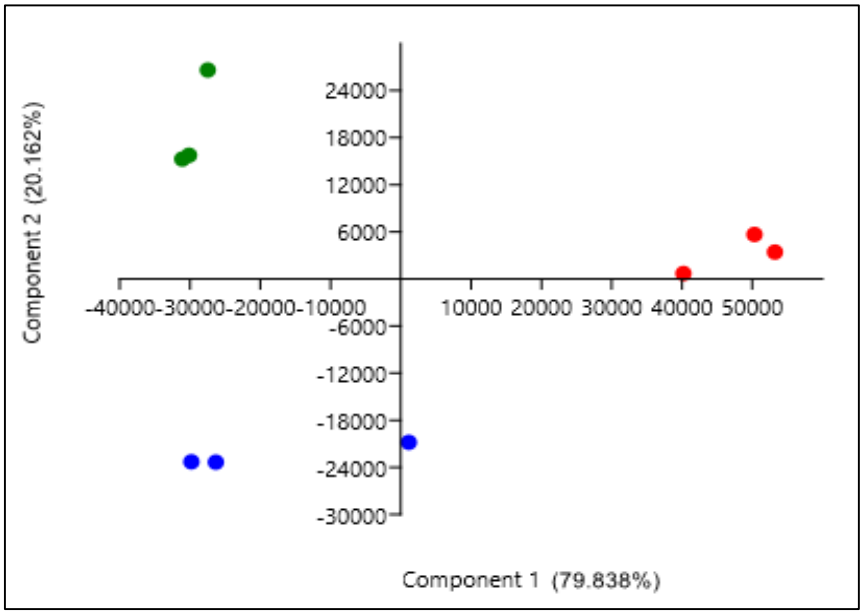

(B)

Figure 3: PCA scatter plots showing the variation between samples and consistency between replicates. Triplicates of *H. alvei* FB1 WT, Δ*halI*::KanR, and Δ*halR*::KanR are represented as green, red, and blue dots, respectively. (A) Samples harvested in early exponential phase. (B) Samples harvested in mid-exponential phase.

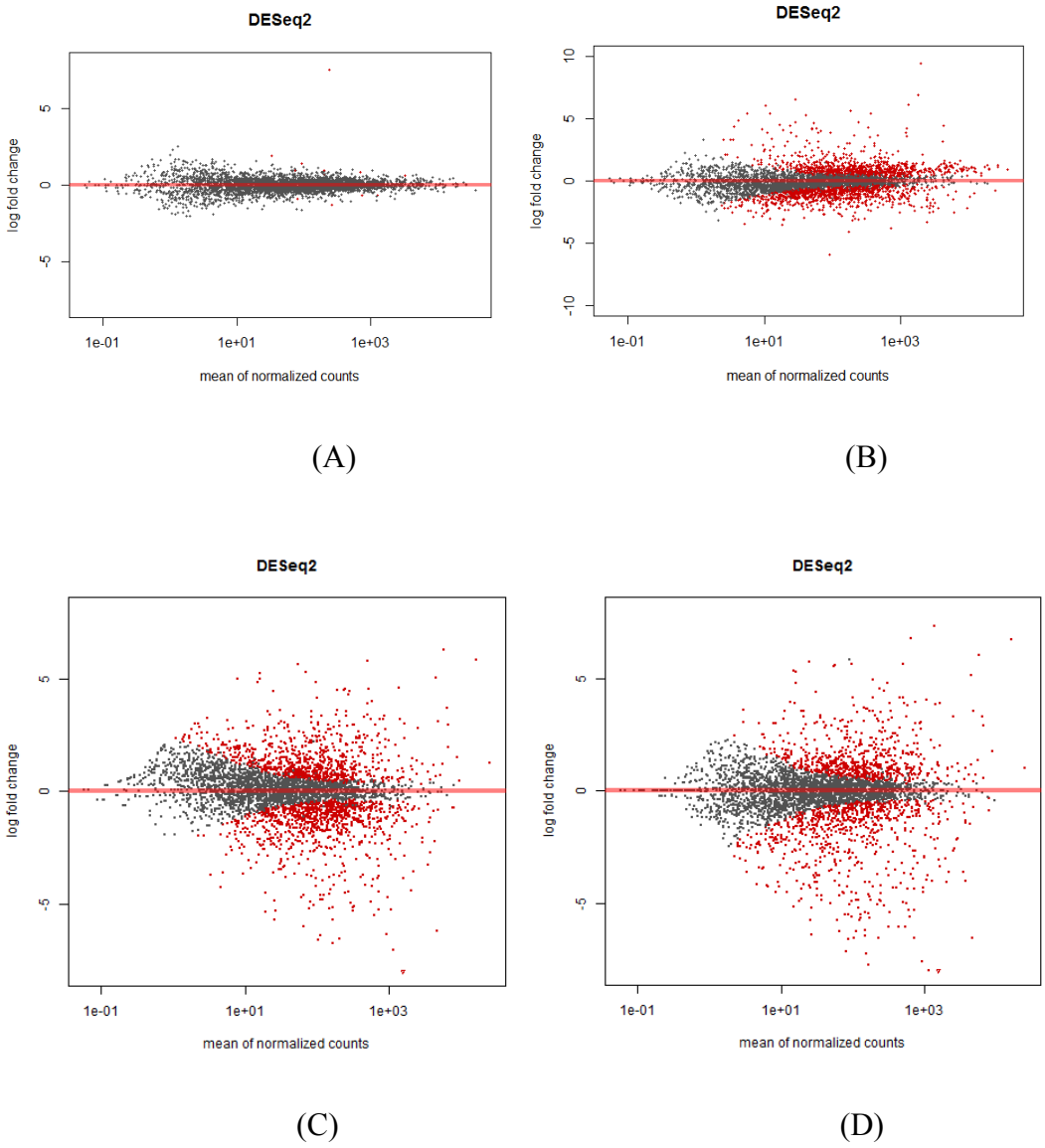

Figure 4: MA plots showing the distribution of DEGs in (A) Δ*halI*::KanR and (B) Δ*halR*::KanR against WT in early exponential phase and (C) Δ*halI*::KanR and (D) Δ*halR*::KanR against WT in mid-exponential phase. Grey dots: genes with $\log_2$ FCs below 1 and above -1; red dots: genes with $\log_2$ FCs above 1 and below -1.

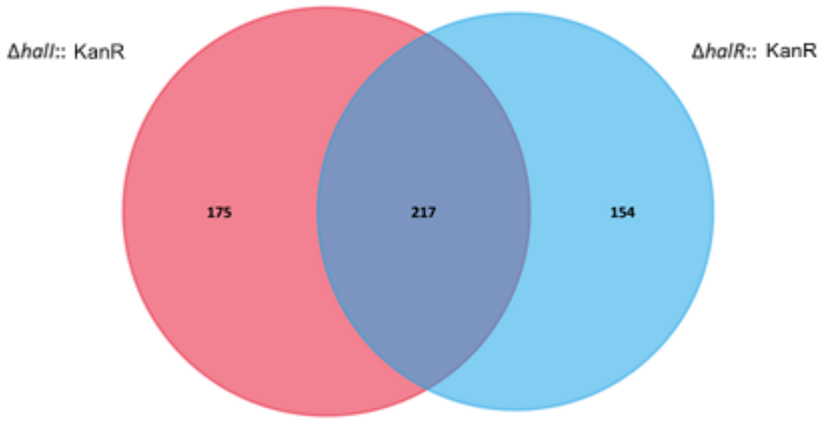

(A)

(B)

Figure 5: Venn diagrams showing the overlapping DEGs between Δ*halI*::KanR and Δ*halR*::KanR mutants in mid-exponential phase. (A) A total of 217 up-regulated genes ($\log_2$ FC > 1, *q*-value < 0.01) are shared between Δ*halI*::KanR (red circle) and Δ*halR*::KanR (blue circle), which contain 175 and 154 unique up-regulated genes, respectively, (B) A total of 273 down-regulated genes ($\log_2$ FC < -1, *q*-value < 0.01) are shared between Δ*halI*::KanR (red circle) and Δ*halR*::KanR (blue circle), which contain 160 and 96 unique down-regulated genes, respectively.

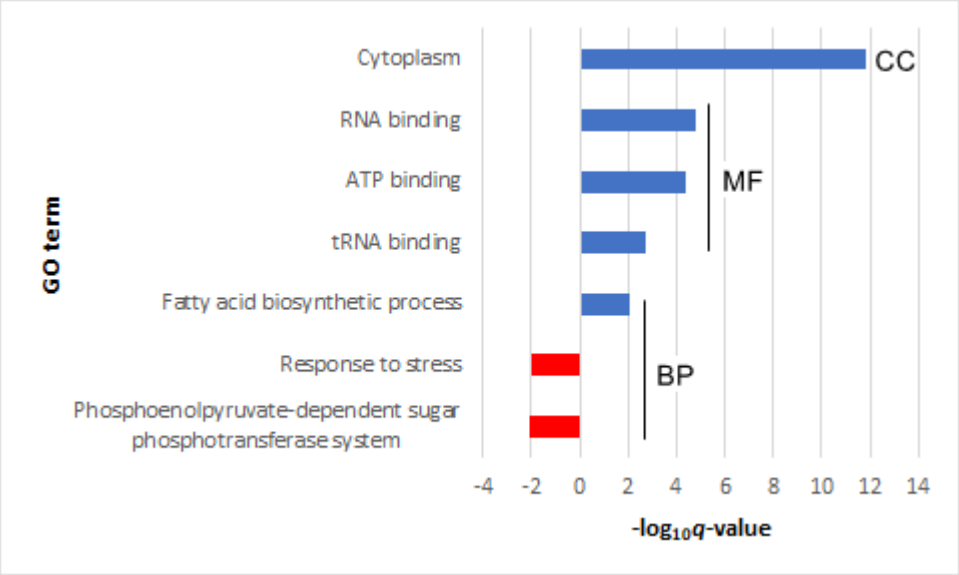

656

657 (A)

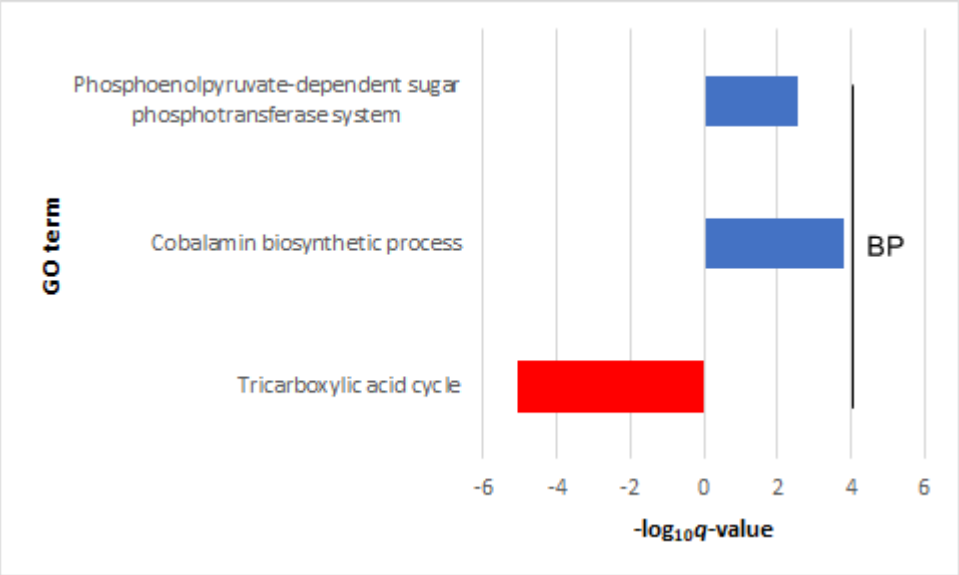

658

659 (B)

660 **Figure 6**: GO enrichment grouping of QS-dependent genes in *halR*::KanR in (A) early exponential phase and
661 (B) mid-exponential phase. CC: Cellular content; MF: Molecular function; BP: Biological process.

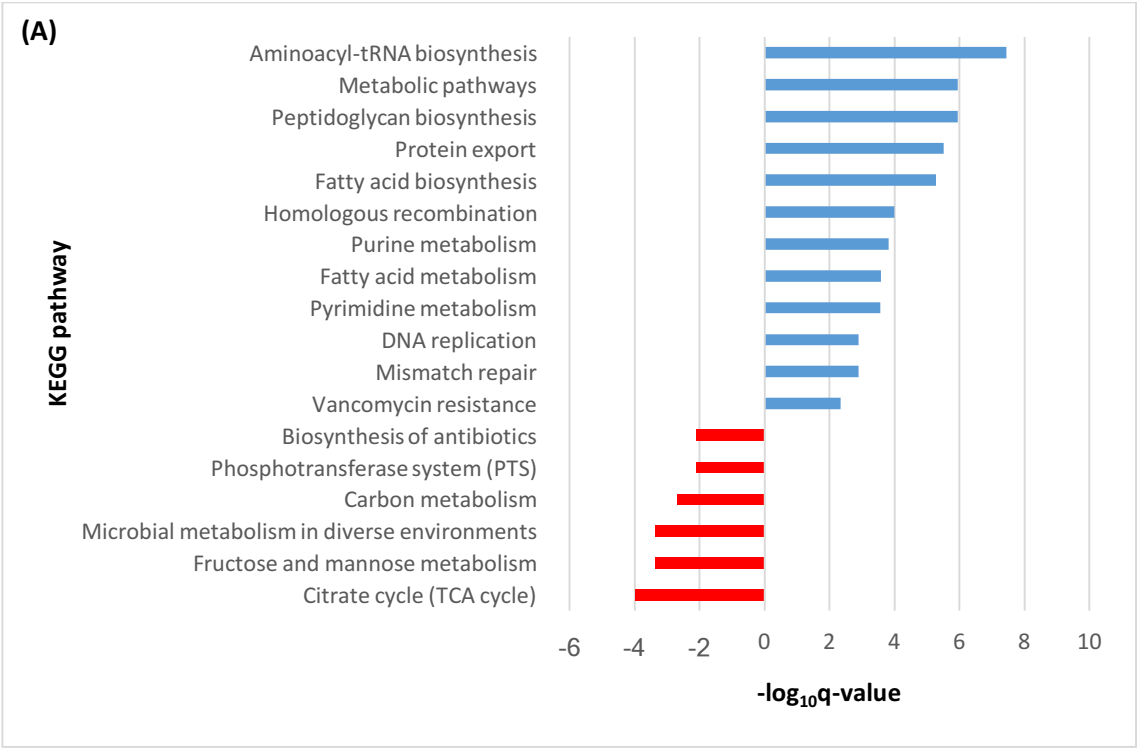
(A)
KEGG pathway
Aminoacyl-tRNA biosynthesis
Metabolic pathways
Peptidoglycan biosynthesis
Protein export
Fatty acid biosynthesis
Homologous recombination
Purine metabolism
Fatty acid metabolism
Pyrimidine metabolism
DNA replication
Mismatch repair
Vancomycin resistance
Biosynthesis of antibiotics
Phosphotransferase system (PTS)
Carbon metabolism
Microbial metabolism in diverse environments
Fructose and mannose metabolism
Citrate cycle (TCA cycle)
-6
-4
-2
0
2
4
6
8
10
-log10q-value

662

(B)

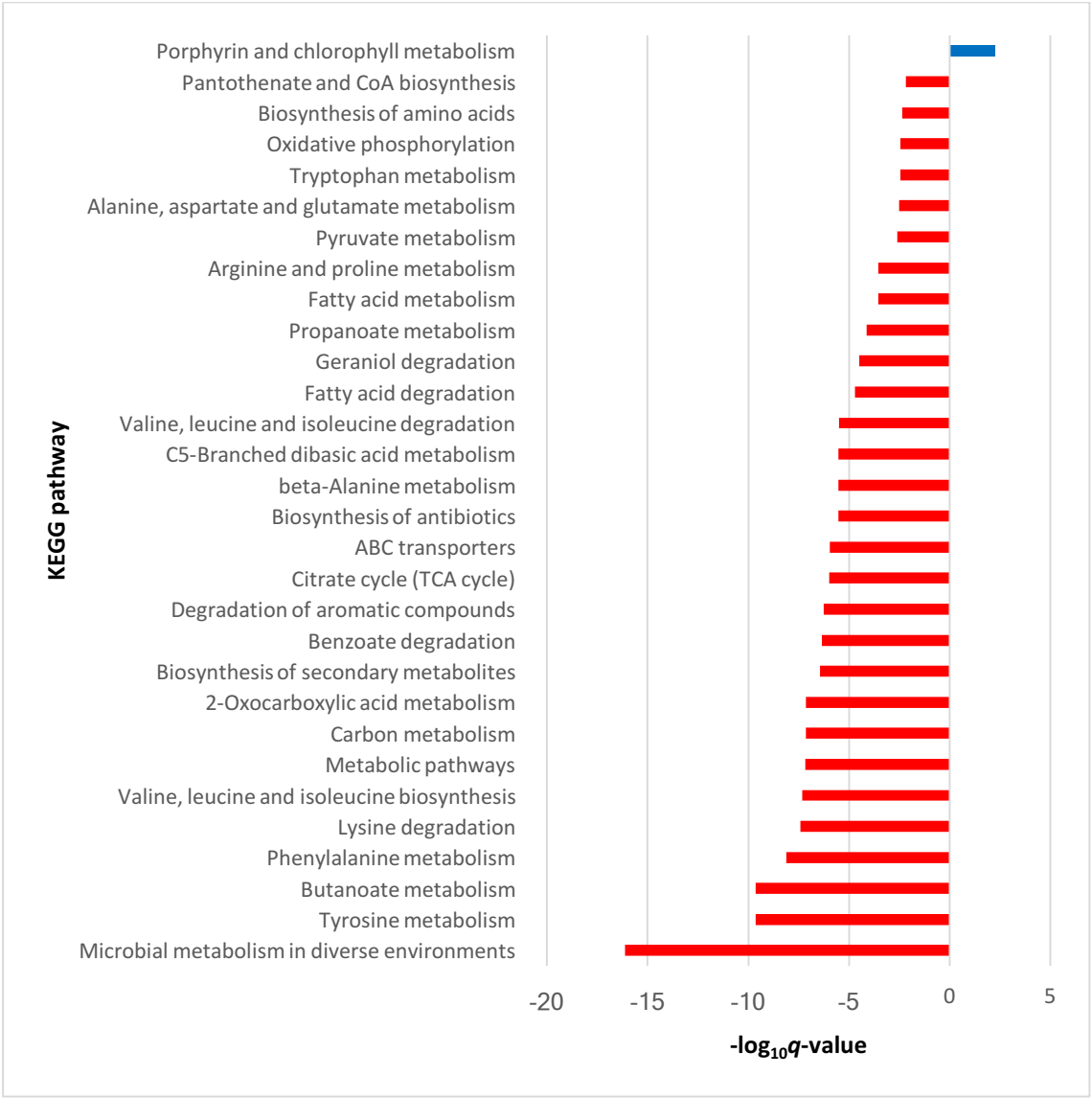
KEGG pathway
Porphyrin and chlorophyll metabolism
Pantothenate and CoA biosynthesis
Biosynthesis of amino acids
Oxidative phosphorylation
Tryptophan metabolism
Alanine, aspartate and glutamate metabolism
Pyruvate metabolism
Arginine and proline metabolism
Fatty acid metabolism
Propanoate metabolism
Geraniol degradation
Fatty acid degradation
Valine, leucine and isoleucine degradation
C5-Branched dibasic acid metabolism
beta-Alanine metabolism
Biosynthesis of antibiotics
ABC transporters
Citrate cycle (TCA cycle)
Degradation of aromatic compounds
Benzoate degradation
Biosynthesis of secondary metabolites
2-Oxocarboxylic acid metabolism
Carbon metabolism
Metabolic pathways
Valine, leucine and isoleucine biosynthesis
Lysine degradation
Phenylalanine metabolism
Butanoate metabolism
Tyrosine metabolism
Microbial metabolism in diverse environments
-20
-15
-10
-5
0
5
-log10q-value

663

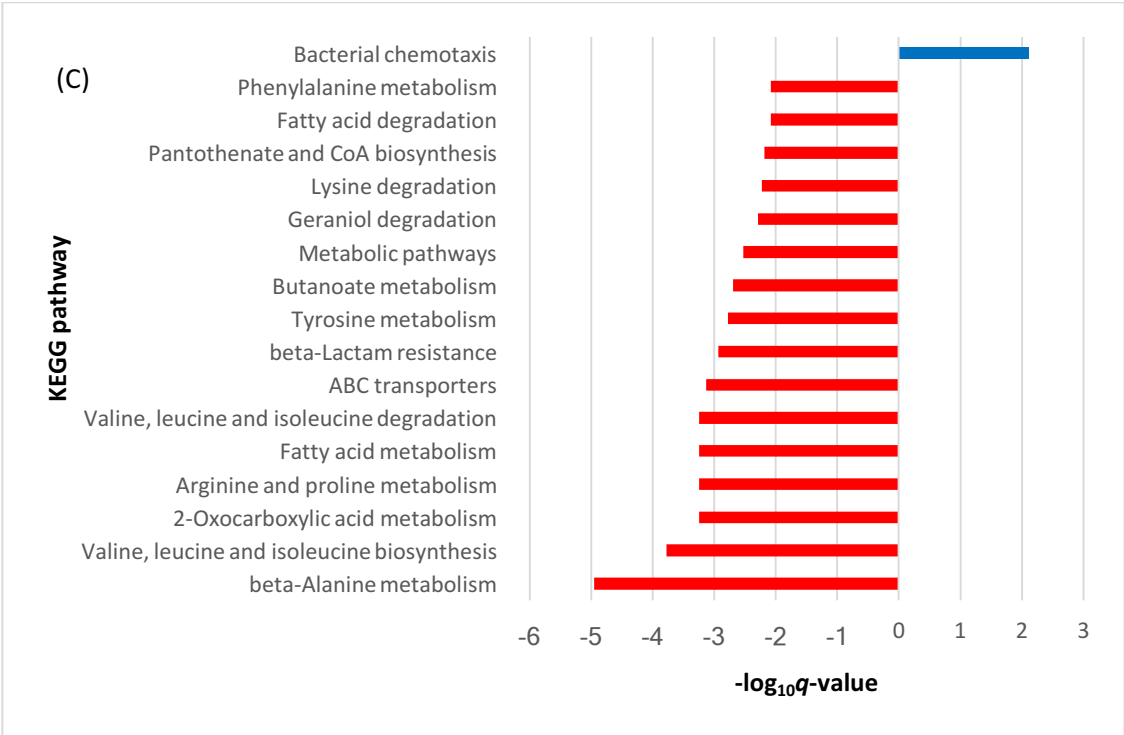

Figure 7: KEGG pathways enriched in (A) Δ*halR*::KanR mutant in early exponential phase, (B) Δ*halR*::KanR mutant in mid-exponential phase, and (C) Δ*halI*::KanR mutant in mid-exponential phase.

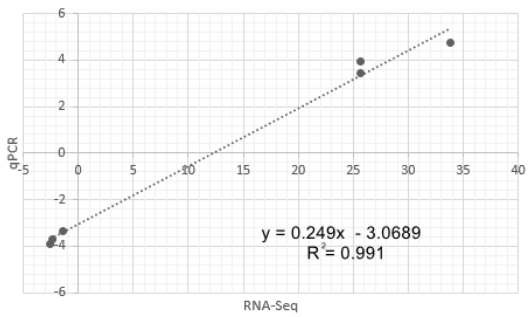

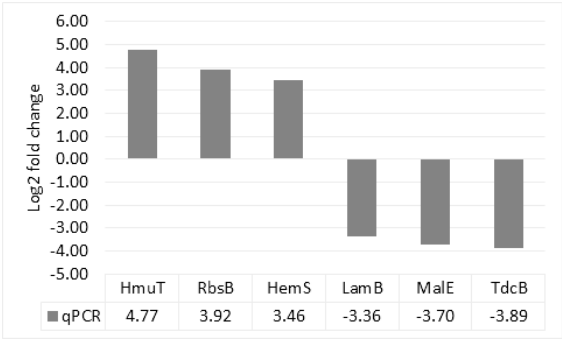

(A) (B)

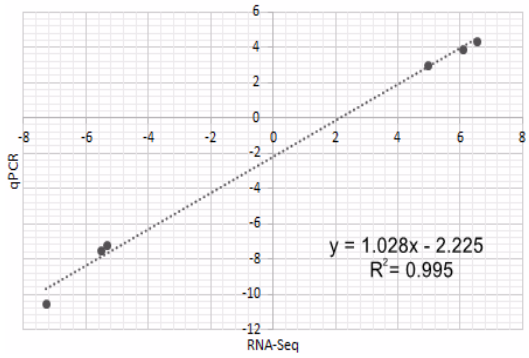

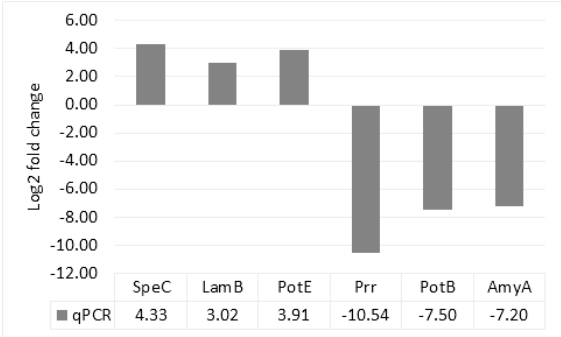

(C) (D)

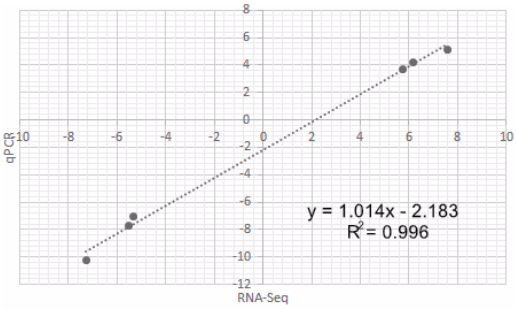

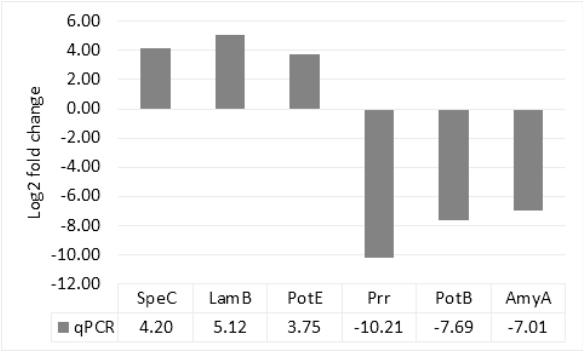

(E) (F)

Figure 8: qPCR validation of RNA-Seq results. Each $\log_2$ ratio of FCs calculated from qPCR was compared with that of the RNA-seq data. (A) Correlation of the FCs between RNA-seq (x-axis) and qPCR (y-axis) of Δ*halR*::KanR in the early exponential phase. (B) Log_2 FCs of Δ*halR*::KanR in the early exponential phase. (C) Correlation of FCs between RNA-seq (x-axis) and qPCR (y-axis) of Δ*halR*::KanR in the mid-exponential phase. (D) Log_2 FCs of Δ*halR*::KanR in the mid-exponential phase. (E) Correlation of fold changes between RNA-seq (x-axis) and qPCR (y-axis) of Δ*halI*::KanR in the mid-exponential phase. (F) Log_2 FCs of Δ*halI*::KanR in the mid-exponential phase.